Gravitomagnetic dynamical friction

Benjamin Cashen,[1,*] Adam Aker,[1,†] and Michael Kesden[1,‡]

[1] *Department of Physics, The University of Texas at Dallas, Richardson, TX 75080, USA*

(Dated: October 7, 2016)

A supermassive black hole moving through a field of stars will gravitationally scatter the stars, inducing a backreaction force on the black hole known as dynamical friction. In Newtonian gravity, the axisymmetry of the system about the black hole's velocity $\mathbf{v}$ implies that the dynamical friction must be anti-parallel to $\mathbf{v}$. However, in general relativity the black hole's spin $\mathbf{S}$ need not be parallel to $\mathbf{v}$, breaking the axisymmetry of the system and generating a new component of dynamical friction similar to the Lorentz force $\mathbf{F} = q\mathbf{v}\times\mathbf{B}$ experienced by a particle with charge q moving in a magnetic field $\mathbf{B}$. We call this new force gravitomagnetic dynamical friction and calculate its magnitude for a spinning black hole moving through a field of stars with Maxwellian velocity dispersion σ, assuming that both v and σ are much less than the speed of light c. We use post-Newtonian equations of motion accurate to $\mathcal{O}(v^3/c^3)$ needed to capture the effect of spin-orbit coupling and also include direct stellar capture by the black hole's event horizon. Gravitomagnetic dynamical friction will cause a black hole with uniform speed to spiral about the direction of its spin, similar to a charged particle spiraling about a magnetic field line, and will exert a torque on a supermassive black hole orbiting a galactic center, causing the angular momentum of this orbit to slowly precess about the black-hole spin. As this effect is suppressed by a factor $(\sigma/c)^2$ in nonrelativistic systems, we expect it to be negligible in most astrophysical contexts but provide this calculation for its theoretical interest and potential application to relativistic systems.

PACS numbers: 98.10+z, 04.70.Bw, 04.25.Nx

I. INTRODUCTION

Chandrasekhar was the first to recognize that a massive perturber moving through a stellar background would scatter stars, resulting in a net deceleration in the direction of its motion known as dynamical friction [1]. Dynamical friction is responsible for many astrophysical phenomena [2] including satellite galaxies inspiraling towards the centers of their host galaxies [3–5], mass segregation of heavy objects in globular clusters [6, 7], the distribution of galaxies within clusters [8, 9], and the migration of planetesimals in protoplanetary disks [10–12]. It also causes supermassive black holes to sink towards the galactic center following a galaxy merger [13–16], helping them to reach sub-parsec separations at which gravitational radiation is effective in promoting black-hole mergers. Dynamical friction also damps out the oscillations of supermassive black holes that have been displaced from the centers of their host galaxies following a gravitational recoil [17–19] produced during a black-hole merger [20].

Dynamical friction can also be interpreted as the gravitational drag force exerted by the effective wake of stars created behind a massive perturber by its gravitational scattering [21–23]. If the stellar background is homogeneous and isotropic in its rest frame, and the perturber is treated as a Newtonian point mass, the system is axisymmetric about the velocity $\mathbf{v}$ of the perturber and the wake produced will be axisymmetric as well. However, if the perturber is a black hole, it can have a spin $\mathbf{S}$ [24] that need not be parallel to $\mathbf{v}$, breaking the axisymmetry of the system. Like a paddle dipped over the side of a canoe, the spin will disturb the wake of the black hole and cause it to deviate from a straight path through the stellar background. As the relative velocities v between supermassive black holes and the stars in their host galaxies are usually much less than the speed of light c, and the distances r between the black holes and these stars is much greater than the gravitational radius $r_g \equiv GM/c^2$ of a black hole of mass M, we will work in the post-Newtonian (PN) approximation [25] in which the equations of motion are expanded in powers of the small parameters $(v/c)^2$ and r_g/r. We will show that the lowest-order spin-dependent terms in the scattering of stars by a supermassive black hole induce a dynamical backreaction force on the black hole in the direction given by $\mathbf{v} \times \mathbf{S}$. In an analogy with the Lorentz force $q\mathbf{v}\times\mathbf{B}$ experienced by a charge q moving through a magnetic field $\mathbf{B}$, we dub this force *gravitomagnetic dynamical friction*. Although there has been extensive work on the spin-dependent two-body problem in general relativity [26–28] as well as some studies of dynamical friction on bodies moving at relativistic speeds [29–32], to our knowledge this paper provides the first calculation of dynamical friction in which gravitomagnetic effects are taken into account. Although the magnitude of the gravitomagnetic contribution to dynamical friction is strongly suppressed compared to the Newtonian one for supermassive black holes in realistic host galaxies, we present this calculation for its theoretical interest and potential applicability to relativistic systems.

In Sec. II, we review how spinning supermassive black

* ben@jwnutritional.com
† axa130531@utdallas.edu
‡ kesden@utdallas.edu

holes scatter stars on hyperbolic orbits in general relativity. In Sec. III, we describe how these results can be used to perform a Monte Carlo calculation of the gravitomagnetic contribution to the coefficient of dynamical friction. In Sec. IV, we present the results of this calculation and explore the how the coefficient depends on the black-hole velocity and spin. A brief summary and discussion of the potential astrophysical applications of gravitomagnetic dynamical friction are provided in Sec. V.

II. POST-NEWTONIAN ORBITAL PRECESSION

The equations of motion for two Newtonian point particles with masses m_1 and m_2 and separation $\mathbf{r}$ can be converted into an effective one-body equation of motion with acceleration

$$\mathbf{a}_N = -\frac{M}{r^2}\hat{\mathbf{r}} \ , \tag{1}$$

where $M \equiv m_1 + m_2$ is the total mass and we use units where $G = c = 1$. In the PN approximation, this Newtonian acceleration is supplemented by higher-order corrections [33]

$$\mathbf{a} = \mathbf{a}_N + \mathbf{a}_{1PN} + \mathbf{a}_{SO} + \ldots \tag{2}$$

where

$$\mathbf{a}_{1PN} = -\frac{M}{r^2}\left\{\hat{\mathbf{r}}\left[(1+3\eta)v^2 - 2(2+\eta)\frac{M}{r} - \frac{3}{2}\eta\dot{r}^2\right] - 2(2-\eta)\dot{r}\mathbf{v}\right\} \tag{3}$$

and

$$\mathbf{a}_{SO} = \frac{1}{r^3}\left\{6\hat{\mathbf{r}}\left[(\hat{\mathbf{r}}\times\mathbf{v})\cdot\left(2\mathbf{S} + \frac{\delta m}{M}\boldsymbol{\Delta}\right)\right] - \left[\mathbf{v}\times\left(7\mathbf{S} + 3\frac{\delta m}{M}\boldsymbol{\Delta}\right)\right] + 3\dot{r}\left[\hat{\mathbf{r}}\times\left(3\mathbf{S} + \frac{\delta m}{M}\boldsymbol{\Delta}\right)\right]\right\} \tag{4}$$

where $\mathbf{v}$ is the relative velocity, $\eta \equiv m_1 m_2/M^2$ is the symmetric mass ratio, $\mathbf{S} \equiv \mathbf{S}_1 + \mathbf{S}_2$ is the total spin, $\delta m \equiv m_1 - m_2$ is the mass difference, and $\boldsymbol{\Delta} \equiv M(\mathbf{S}_2/m_2 - \mathbf{S}_1/m_1)$. These expressions simplify in the limit that the supermassive black hole is much more massive than the stars it scatters ($m_1 \gg m_2$) in which case $\eta \to 0$, $\mathbf{S} \to \mathbf{S}_1$, $\delta m/M \to 1$, $\boldsymbol{\Delta} \to -\mathbf{S}$, and (with the help of some vector identites)

$$\mathbf{a}_{SO} \to -\frac{2M^2}{r^3}\mathbf{v}\times[-\boldsymbol{\chi} + 3(\hat{\mathbf{r}}\cdot\boldsymbol{\chi})\hat{\mathbf{r}}] \tag{5}$$

where $\boldsymbol{\chi} \equiv \mathbf{S}_1/m_1^2$ is the dimensionless spin of the black hole.

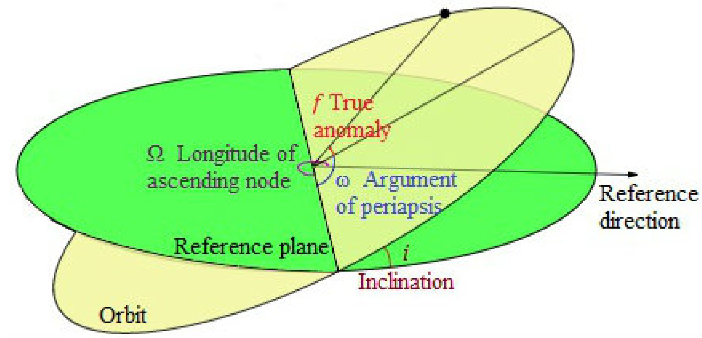

FIG. 1. A Keplerian orbit in three dimensions, showing the angles that define its orientation in space: the inclination i, the argument of periapsis ω, and the longitude of ascending node Ω. The true anomaly f specifies the position of a star on its orbit with $f = 0$ at pericenter.

Dynamical friction is caused by the gravitational scattering of stars by the black hole as it moves through the stellar background. These stars are gravitationally unbound to the black hole; they approach from large distances, reach orbital pericenter, and then return to infinity. Well before and after each scattering event, the PN accelerations given by Eqs. (3) and (4) are highly subdominant compared to the Newtonian acceleration $\mathbf{a}_N$ and the stellar orbits are well described by Keplerian hyperbolae. In addition to its semi-major axis a and eccentricity e, a hyperbolic orbit is specified by its inclination i, argument of periapsis ω, and longitude of ascending node Ω as shown in Fig. 1. We choose the reference plane to correspond to the equatorial plane perpendicular to the spin of the black hole implying that the inclination i is the angle between the orbital angular momentum of the star and the spin of the black hole.

Although the five orbital elements a, e, i, ω, and Ω are conserved by the Newtonian acceleration $\mathbf{a}_N$, in the Kerr geometry of a spinning black hole, conservation of the energy E, z-component of the angular momentum L_z, and Carter constant Q [34] only require that the first three orbital elements remain unchanged by the scattering event. The 1PN acceleration $\mathbf{a}_{1PN}$ given by Eq. (3) causes the argument of periapsis for a star on a parabolic orbit with specific orbital angular momentum L to precess by an amount

$$\Delta\omega_{1PN} = 6\pi\left(\frac{M}{L}\right)^2 \tag{6}$$

as was famously shown by Einstein to account for the anomalous precession of Mercury's orbit [25]. Although this pericenter precession should induce a small correction to non-relativistic calculations of dynamical friction, it does not depend on the black-hole spin and thus cannot generate the gravitomagnetic dynamical friction that is our concern in this paper.

The 1.5PN spin-orbit correction to the acceleration $\mathbf{a}_{SO}$ causes both the argument of periapsis and the lon-

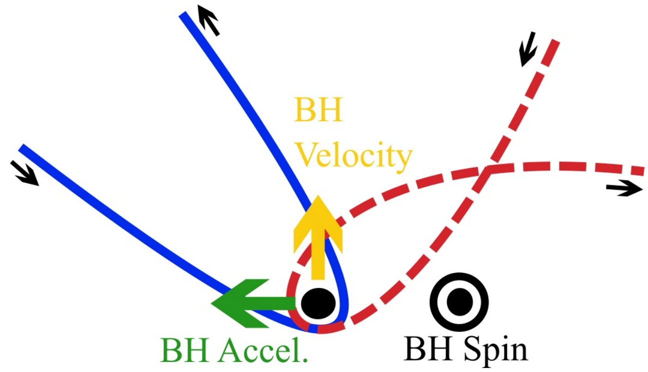

FIG. 2. Gravitomagnetic dynamical friction caused by spin-dependent precession of the argument of periapsis $\Delta\omega_{SO}$. A black hole with velocity directed towards the top of the page (yellow arrow) will encounter more stars with relative velocities directed towards the bottom of the page as indicated by the downwards black arrows on both orbits. The black-hole spin is directed out of the page. Eq. (7a) implies that stars on prograde orbits ($\cos i > 0$, solid blue curve) will experience negative spin-dependent pericenter precession and thus a smaller deflection than stars on retrograde orbits ($\cos i < 0$, dashed red curve). The vector sum of the two outwards directed arrows on these orbits has a component directed to the right side of the page yielding a net backreaction force on the black hole directed to the left (leftwards green arrow).

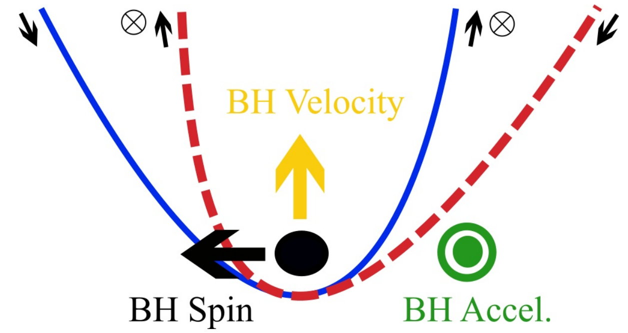

FIG. 3. Gravitomagnetic dynamical friction caused by precession of the longitude of ascending node $\Delta\Omega_{SO}$. The black-hole velocity (yellow arrow) is directed towards the top of the page as in Fig. 2, but the black-hole spin (black arrow) is now directed towards the left of the page making the solid blue and dashed red curves correspond to polar orbits with orbital angular momenta directed out of and into the page respectively. Precession of the longitude of ascending node causes the orbital angular momenta to precess about the black-hole spin, deflecting stars on both orbits into the page as indicated by the $\otimes$ symbols on these orbits as they recede from the black hole. The backreaction force on the black hole is directed out of the page as shown by the green $\odot$ symbol.

gitude of ascending node to precess by [35]

$$\Delta\omega_{SO} = -12\pi\chi\cos i\left(\frac{M}{L}\right)^3 , \tag{7a}$$

$$\Delta\Omega_{SO} = 4\pi\chi\left(\frac{M}{L}\right)^3 . \tag{7b}$$

These two changes to the orbital elements during a scattering event each contribute to gravitomagnetic dynamical friction. Let us first consider the effects of spin-dependent pericenter precession as illustrated in Fig. 2 where the velocity of the black hole is directed towards the top of the page and the black-hole spin is directed out of the page. The negative sign in Eq. (7a) implies that stars passing on the left side of the black hole (prograde orbits with $\cos i > 0$) will be scattered by smaller angles than those passing on the right side (retrograde orbits with $\cos i < 0$). The black hole will therefore preferentially scatter stars towards the right side of the page and experience a backreaction force to the left. This force is anti-aligned with $\mathbf{v}\times\mathbf{S}$ allowing us to identify it as gravitomagnetic dynamical friction.

Let us next consider the effects of precession of the longitude of ascending node as illustrated in Fig. 3. The velocity of the black hole is again directed towards the top of the page, but the black-hole spin is now directed to the left side of the page. This choice allows the plane of the page to correspond to the initial orbital plane of polar orbits. The solid blue and dashed red orbits have angular momenta directed out of and into the page respectively, which according to Eq. (7b) will precess about the black-hole spin as stars are scattered. In both cases, the final orbital plane will dip into the top of the page causing stars to be preferentially scattered below the plane of the page. This induces a backreaction force on the black hole out of the page in the direction of $\mathbf{v}\times\mathbf{S}$ as expected for a gravitomagnetic force. As this contribution to the gravitomagnetic dynamical friction has the opposite sign of that from the spin-dependent pericenter precession as shown in Fig. 2, a quantitative calculation is needed to determine which effect predominates. We will provide such a calculation in Sec. III.

We conclude this section by briefly considering relativistic corrections beyond 1.5 PN order. Black-hole spin induces a mass-quadrupole moment [36, 37] which in turn generates precession of the pericenter and longitude of ascending node at 2PN order [35]

$$\Delta\omega_Q = -\frac{3\pi\chi^2}{2}(1-5\cos^2 i)\left(\frac{M}{L}\right)^4 , \tag{8a}$$

$$\Delta\Omega_Q = 3\pi\chi^2\cos i\left(\frac{M}{L}\right)^4 . \tag{8b}$$

These terms have the opposite parity under reflection through the equatorial plane ($\cos i \to -\cos i$) of the 1.5 PN terms given by Eq. (7) implying that, like the 1PN term of Eq. (6), they will not give rise to gravitomagnetic dynamical friction. We have confirmed this result by showing that including these terms does not affect our subsequent numerical calculations.

III. COEFFICIENT OF GRAVITOMAGNETIC DYNAMICAL FRICTION

In this section, we calculate the component of the coefficient $\langle \Delta \mathbf{v} \rangle$ responsible for gravitomagnetic dynamical friction. This coefficient specifies the time rate of change of the black hole's velocity, i.e. its acceleration. Following Chandrasekhar's original treatment of dynamical friction [1], we assume that the stellar distribution function far from the black hole is spatially homogeneous and has a Maxwellian velocity distribution

$$f(\mathbf{x}, \mathbf{v}') = \frac{n}{(2\pi\sigma^2)^{3/2}} e^{-v'^2/2\sigma^2} \ , \tag{9}$$

where n is the stellar number density and σ is the one-dimensional velocity dispersion. If the black hole has a velocity $\mathbf{v}'_{BH}$ in this mean stellar rest frame, we can perform a change of variables $\mathbf{v} \equiv \mathbf{v}' - \mathbf{v}'_{BH}$ to find a star's velocity in the black-hole rest frame. In this frame, we can express the Cartesian components of the stellar velocity $\mathbf{v}$ as

$$v_x = v_r \sin\theta \cos\phi - \frac{L}{r}(\cos\phi_v \sin\phi + \sin\phi_v \cos\theta \cos\phi) \tag{10a}$$

$$v_y = v_r \sin\theta \sin\phi + \frac{L}{r}(\cos\phi_v \cos\phi - \sin\phi_v \cos\theta \sin\phi) \tag{10b}$$

$$v_z = v_r \cos\theta + \frac{L}{r} \sin\phi_v \sin\theta \tag{10c}$$

where (θ, ϕ) is the star's angular position defined such that $\mathbf{v}'_{BH}$ is along the z axis, v_r is the radial velocity, L is the magnitude of the orbital angular momentum, and ϕ_v is an azimuthal angle about the radial direction defined such that the tangential component of $\mathbf{v}$ is purely azimuthal for $\phi_v = 0$. These new variables, the distribution function (9), and the additional definition $\mu \equiv \cos\theta$ allow the differential flux of stars entering a sphere of radius $r \gg GM/\sigma^2$ to be expressed as

$$\frac{d^5F}{d\mu d\phi dv_r dL d\phi_v} = \frac{nLv_r}{(2\pi\sigma^2)^{3/2}} e^{-|\mathbf{v}+\mathbf{v}'_{BH}|^2/2\sigma^2} \ . \tag{11}$$

If a star with mass m_* scattered by a black hole of mass M experiences a velocity change $\Delta\mathbf{v}_*(\mu, \phi, v_r, L, \phi_v)$, conservation of linear momentum implies that the velocity of the black hole will be changed by an amount

$$\Delta\mathbf{v}_{BH} = -(m_*/M)\Delta\mathbf{v}_* \ . \tag{12}$$

Eq. (11) then indicates that the coefficient of dynamical friction $\langle \Delta \mathbf{v} \rangle$ will be

$$\begin{aligned} \langle \Delta \mathbf{v} \rangle &= \int \Delta\mathbf{v}_{BH} \frac{d^5F}{d\mu d\phi dv_r dL d\phi_v} d\mu \, d\phi \, dv_r \, dL \, d\phi_v \\ &= -\frac{m_* n}{M(2\pi\sigma^2)^{3/2}} e^{-v'^2_{BH}/2\sigma^2} \int \Delta\mathbf{v}_* L v_r \\ &\quad \times e^{-(v_r^2 + 2v_r v'_{BH}\mu)/2\sigma^2} d\mu \, d\phi \, dv_r \, dL \, d\phi_v \end{aligned} \tag{13}$$

where the limits of integration are $-1 < \mu < +1$, $0 < \phi < 2\pi$, $v_r < 0$, $L > 0$, and $0 < \phi_v < 2\pi$.

To evaluate this integral, we must first derive an expression for the change in stellar velocity $\Delta\mathbf{v}_*$. Qualitatively, there are two possibilities: either the star is directly captured by the black hole's event horizon or it is scattered by the black hole and returns to infinity. Let us first consider direct capture by the black hole. If the stellar velocity is given by Eq. (10), the star's specific orbital angular momentum $\mathbf{L} = \mathbf{r} \times \mathbf{v}$ will be

$$L_x = L(\sin\phi_v \sin\phi - \cos\phi_v \cos\theta \cos\phi) \tag{14a}$$

$$L_y = -L(\sin\phi_v \cos\phi + \cos\phi_v \cos\theta \sin\phi) \tag{14b}$$

$$L_z = L \cos\phi_v \sin\theta \ . \tag{14c}$$

If we choose without loss of generality for the black-hole spin direction $\hat{\mathbf{S}}$ to lie in the xz plane at an angle θ_S with respect to the z axis, the inclination will be

$$\begin{aligned} \cos i &= \hat{\mathbf{L}} \cdot \hat{\mathbf{S}} \\ &= \cos\theta_S \cos\phi_v \sin\theta \\ &\quad + \sin\theta_S(\sin\phi_v \sin\phi - \cos\phi_v \cos\theta \cos\phi) \ . \end{aligned} \tag{15}$$

The values $L_{\rm mb\pm}(\chi)$ of the orbital angular momentum below which stars on parabolic orbits in the equatorial plane of the black hole are captured by the black hole can be found from the geodesic equations; the approximation of strictly parabolic orbits (specific energy $E = 1$) for both capture and scattering is valid since the star's velocities at infinity $v \sim \sigma \ll c$ are highly nonrelativistic. For non-spinning black holes ($\chi = 0$), $L_{\rm mb\pm} = 4M$ since the inclination is undefined, while for maximally spinning black holes ($\chi = 1$), $L_{\rm mb+} = 2M$ for prograde orbits ($\cos i = +1$) while $L_{\rm mb-} = 2(1+\sqrt{2})M$ for retrograde orbits ($\cos i = -1$) [38]. We can calculate $L_{\rm mb}$ for non-equatorial orbits by finding the value of L for which there is an unstable circular geodesic with $E = 1$, $L_z = L\cos i$, and $Q = (L\sin i)^2$; $L_{\rm mb}$ is a monotonically increasing function of the inclination i with $L_{\rm mb+} \leq L_{\rm mb} \leq L_{\rm mb-}$. When a star is captured, all of its linear momentum is transferred to the black hole and $\Delta\mathbf{v}_* = -\mathbf{v}$. Since all stars with $L < L_{\rm mb+}$ are captured, the net linear momentum they contribute to the black hole must be anti-aligned with $\mathbf{v}'_{BH}$ and thus cannot contribute to the gravitomagnetic dynamical friction. The prograde marginally bound orbital angular momentum $L_{\rm mb+}$ can thus serve as an effective lower limit for the integral in Eq. (13).

The second possible fate of the star is that it is scattered by the black hole and returns to infinity. The much larger mass of the black hole ($M \gg m_*$) implies that the star's speed is nearly conserved ($v_i \simeq v_f$). In Newtonian gravity, a star with specific energy E and specific angular momentum L will have eccentricity

$$e = \left[1 + 2E\left(\frac{L}{GM}\right)^2\right]^{1/2} \tag{16}$$

and be scattered by an angle

$$\delta = 2\cos^{-1}(-e^{-1}) - \pi \ , \tag{17}$$

where we have temporarily restored the factors of G and c for clarity of presentation. Stars described by the distribution function of Eq. (9) have $E \sim \sigma^2$, and if they are to experience significant spin-orbit coupling according to Eq. (7) must have $L \gtrsim GM/c$. This implies eccentricities $e - 1 \simeq (\sigma/c)^2 \ll 1$ and deflections $\delta \simeq \pi$. We can therefore approximate that in the absence of precession, scattering will change a star's velocity by $\Delta\mathbf{v}_* = -2\mathbf{v}$.

Precession will change the direction of the final stellar velocity $\mathbf{v}_f$ so that it is no longer anti-aligned with the initial velocity $\mathbf{v}$ and thus $\Delta\mathbf{v}_* = \mathbf{v}_f - \mathbf{v} \neq -2\mathbf{v}$. To determine $\Delta\mathbf{v}_*(\mu, \phi, v_r, L, \phi_v)$, we begin by calculating $\mathbf{v}$ and $\mathbf{L}$ from Eqs. (10) and (14) in the limit $r \to \infty$ appropriate for the initial quantities at large separations. To determine the components of these vectors in the "spin frame" in which the equatorial plane perpendicular to the black-hole spin serves as the reference plane shown in Fig. 1, we rotate them by an angle $-\theta_S$ about the y axis. The stellar inclination i (which remains unchanged by precession) is given by Eq. (15). The unit vector $\hat{\mathbf{n}} = (\hat{\mathbf{S}} \times \hat{\mathbf{L}})/\sin i$ points along the line of ascending node and its azimuthal angle in spherical coordinates of the spin frame is the initial longitude of ascending node Ω. Since the initial stellar velocity $\mathbf{v}$ points towards pericenter for parabolic ($e = 1$) orbits, the argument of periapsis ω will be the azimuthal angle of $\mathbf{v}$ in a frame with $\hat{\mathbf{n}}$ along the x axis and $\hat{\mathbf{L}}$ along the z axis as shown in Fig. 1.

Once we have determined the initial orbital elements Ω, i, and ω in the spin frame, the final orbital elements are

$$\Omega_f = \Omega + \Delta\Omega_{SO} \ , \tag{18a}$$
$$i_f = i \ , \tag{18b}$$
$$\omega_f = \omega + \Delta\omega_{SO} \ , \tag{18c}$$

where $\Delta\omega_{SO}$ and $\Delta\Omega_{SO}$ are given by Eq. (7). The final stellar velocity $\mathbf{v}_f$ in the spin frame is found by successively rotating $-v\hat{\mathbf{x}}$ by the three Euler angles given in Eq. (18): we rotate first by Ω_f about the black-hole spin $\mathbf{S}$, next by i_f about the line of ascending node $\hat{\mathbf{n}}$, and finally by ω_f about the orbital angular momentum $\mathbf{L}$. We then calculate the change in stellar velocity $\Delta\mathbf{v}_* = \mathbf{v}_f - \mathbf{v}$ and rotate by an angle θ_S about the y axis to transform back from the spin frame to the black-hole rest frame. We use this $\Delta\mathbf{v}_*$ in Eq. (13) and Monte Carlo methods to perform the required integration, allowing us to calculate the coefficient of dynamical friction.

IV. RESULTS

In Fig. 4, we show the coefficient of gravitomagnetic dynamical friction $\langle \Delta v_\perp \rangle$ as a function of $L_{\rm max}$, the upper limit of the integral over L in Eq. (13). We use fiducial parameters $n = 10^6\,{\rm pc}^{-3}$, $M = 10^6\,M_\odot$, $m_* = M_\odot$, and $\sigma = 100\,{\rm km/s}$ typical of a supermassive black hole moving in a galactic nuclear star cluster. We measure this acceleration using the unusual units of km/s/Gyr as galactic speeds and dynamical times are typically measured in km/s and Gyr respectively. All stars with $L \leq L_{\rm mb+} = 2M$ are directly captured by the black hole implying by symmetry that they provide zero net contribution to the gravitomagnetic dynamical friction. As $L_{\rm max}$ increases from $L_{\rm mb+}$ to $L_{\rm mb-}$, stars on orbits with increasing inclination manage to escape to infinity and exert a net transverse force on the supermassive black hole as indicated by the dashed purple curve in Fig. 4. This curve reaches a maximum at $L_{\rm max} \simeq 4.875$ quite close to the maximum orbital angular momentum for capture from retrograde orbits $L_{\rm mb-} = 2(1 + \sqrt{2})$. The precession angles $\Delta\omega$ and $\Delta\Omega$ diverge for true marginally bound Kerr geodesics, unlike the 1.5PN results given by Eq. (7), but greater precession would not necessarily lead to larger gravitomagnetic dynamical friction. The effect would be eliminated if ω_f and Ω_f were fully randomized. As it would be computationally prohibitive to solve the geodesic equations for each star in our Monte Carlo simulation, we rely on the 1.5PN results which should provide a reasonable approximation for values of L modestly above the marginally

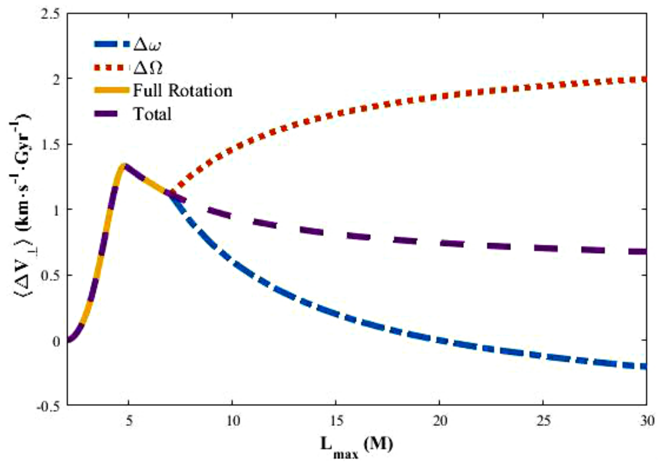

FIG. 4. The component of the coefficient of dynamical friction $\langle \Delta v_\perp \rangle$ perpendicular to the black-hole velocity $\mathbf{v}'_{BH}$ as a function of $L_{\rm max}$, the upper limit of the integral over the orbital angular momentum L in Eq. (13). The black hole has a maximal spin ($\chi = 1$) perpendicular to its velocity ($\theta_s = \pi/2$). The speed of the black hole is equal to the 1D stellar velocity dispersion ($v'_{BH} = \sigma$) and all other parameters are fixed at the fiducial values listed in the text. The solid yellow curve in the range $2M < L < 7M$ shows the total contribution to the gravitomagnetic dynamical friction using the exact Euler rotations to relate the stellar orbits before and after scattering. For $L > 7M$ we linearize in the precession angles $\Delta\omega_{SO}$ and $\Delta\Omega_{SO}$ given by Eq. (7) allowing us to show their separate contributions with the dot-dashed blue and dotted orange curves respectively. The dashed purple curve shows the total contribution which converges for $L_{\rm max} \gtrsim 30M$.

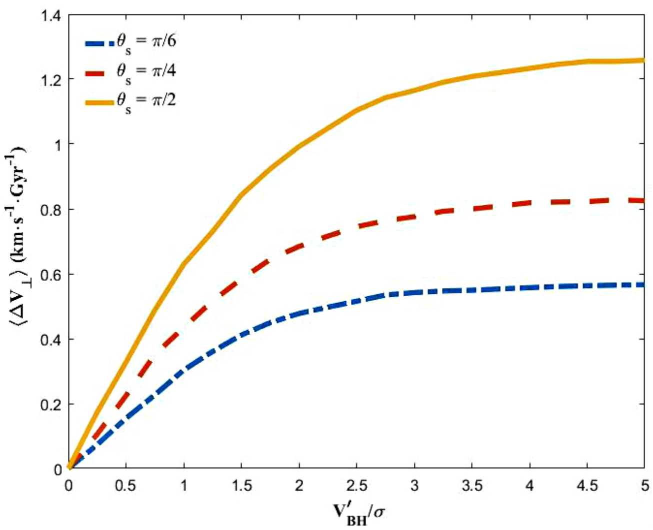

FIG. 5. The coefficient of gravitomagnetic dynamical friction $\langle v_\perp \rangle$ as a function of the ratio v'_{BH}/σ between the speed of the black-hole and the stellar velocity dispersion. Three different values of the angle θ_S between the black-hole spin and velocity are shown: $\pi/2$ (solid yellow curve), $\pi/4$ (dashed orange curve), and $\pi/6$ (dot-dashed blue curve).

bound values. For $L_{\rm mb+} < L < L_{\rm lin} = 7M$, we use the exact rotations specified by the Euler angles of Eq. (7) to calculate the velocity change $\Delta \mathbf{v}_*$ of each star, but for higher values of L where the precession angles are smaller we linearize in these angles to remove the dominant Newtonian contribution to dynamical friction and speed up the convergence of our Monte Carlo integration. This linearization allows us to separate the contributions from apsidal and nodal precession which partially cancel as anticipated by Figs. 2 and 3. Our results converge for $L_{\rm max} \gtrsim 30M$ because the spin-orbit acceleration given by Eq. (4) falls off more rapidly than the inverse-square law.

We can obtain a crude estimate for the coefficient of gravitomagnetic dynamical friction $\langle \Delta v_\perp \rangle$ by assuming that it is comparable to the contribution to the Newtonian coefficient of dynamical friction $\langle \Delta v_\parallel \rangle$ from stars with orbital angular momenta $L \lesssim L_{\rm max} \sim M$ at which the spin-orbit precession of Eq. (7) is significant. In the limit that $v'_{BH},\ \sigma \ll c$, we estimate (using Eq. (5.20) of Merritt [35]) that

$$\begin{aligned}\langle \Delta v_\perp \rangle &\simeq -\frac{2\pi G^2 n M m_*}{c^2}\left(\frac{L_{\rm max}}{M}\right) K\left(\frac{v'_{BH}}{\sqrt{2}\sigma}\right) \\ &\simeq -1.3 \text{ km/s/Gyr } \left(\frac{n}{10^6 \text{ pc}^{-3}}\right)\left(\frac{M}{10^6\ M_\odot}\right) \\ &\quad \times \left(\frac{m_*}{M_\odot}\right)\left(\frac{L_{\rm max}}{M}\right) K\left(\frac{v'_{BH}}{\sqrt{2}\sigma}\right) , \end{aligned} \tag{19}$$

where

$$K(x) \equiv \frac{(2x^2-1)\text{erf}(x) + x\ \text{erf}'(x)}{2x^2} , \tag{20}$$

and erf and erf$'$ are the error function and its first derivative. This function has the limiting behavior $K(x) \simeq 4x/(3\sqrt{\pi})$ for $x \ll 1$ and $K(x) \simeq 1$ for $x \gg 1$. We show the coefficient of gravitomagnetic dynamical friction $\langle v_\perp \rangle$ as a function of the ratio v'_{BH}/σ in Fig. 5. Our estimate (19) provides the correct order of magnitude for $L_{\rm max} \sim M$. Furthermore, $\langle v_\perp \rangle$ depends linearly on the black-hole velocity for $v'_{BH} \ll \sigma$ and asymptotes to a constant value for $v'_{\rm BH} \gg \sigma$ as predicted by Eq. (20).

We can compare gravitomagnetic dynamical friction to Newtonian dynamical friction for the same stellar distribution function

$$\begin{aligned}\langle \Delta v_\parallel \rangle &= -\frac{4\pi G^2 n M m_* \ln\Lambda}{\sigma^2} H\left(\frac{v'_{BH}}{\sqrt{2}\sigma}\right) \\ &= -2.4\times 10^7 \text{ km/s/Gyr } \left(\frac{n}{10^6 \text{ pc}^{-3}}\right)\left(\frac{M}{10^6\ M_\odot}\right) \\ &\quad \times \left(\frac{m_*}{M_\odot}\right)\left(\frac{\sigma}{100 \text{ km/s}}\right)^{-2} \ln\Lambda\ H\left(\frac{v'_{BH}}{\sqrt{2}\sigma}\right) , \end{aligned} \tag{21}$$

where the Coulomb logarithm $\ln\Lambda \sim 10$ and

$$H(x) \equiv \frac{\text{erf}(x) - x\ \text{erf}'(x)}{2x^2} \tag{22}$$

has the limiting behavior $H(x) \simeq 2x/(3\sqrt{\pi})$ for $x \ll 1$ and $H(x) \simeq 1/(2x^2)$ for $x \gg 1$ [35]. Taking the ratio of Eqs. (19) and (21), we find

$$\frac{\langle \Delta v_\perp \rangle}{\langle \Delta v_\parallel \rangle} \simeq \frac{K}{2H\ln\Lambda}\left(\frac{L_{\rm max}}{M}\right)\left(\frac{\sigma}{c}\right)^2 \tag{23}$$

which has the limiting behavior

$$\lim_{v'_{\rm BH}\to 0} \frac{\langle \Delta v_\perp \rangle}{\langle \Delta v_\parallel \rangle} = \frac{1}{\ln\Lambda}\left(\frac{L_{\rm max}}{M}\right)\left(\frac{\sigma}{c}\right)^2 , \tag{24a}$$

$$\lim_{v'_{\rm BH}\to c} \frac{\langle \Delta v_\perp \rangle}{\langle \Delta v_\parallel \rangle} = \frac{1}{2\ln\Lambda}\left(\frac{L_{\rm max}}{M}\right)\left(\frac{v'_{BH}}{c}\right)^2 . \tag{24b}$$

Although gravitomagnetic dynamical friction is suppressed by a factor $(\sigma/c)^2 \ll 1$ compared to Newtonian dynamical friction in the nonrelativistic limit, as the black-hole velocity approaches the speed of light these two effects become comparable.

We show how the coefficient of gravitomagnetic dynamical friction $\langle \Delta v_\perp \rangle$ depends on the black-hole spin in Figs. 6 and 7. Fig. 6 shows the dependence on the dimensionless spin magnitude χ which appears approximately linear for $\chi \lesssim 0.7$ but then grows more steeply as one approaches the maximal spin limit $\chi = 1$. Although the precession angles given by Eq. (7) are linear in the dimensionless spin χ, this linearity is only preserved for contributions to $\langle \Delta v_\perp \rangle$ with $L > L_{\rm lin}$ for which we linearize the Euler rotations in these angles. The nonlinearity in both these rotations and the spin dependence of the limits $L_{\rm mb}$ on marginally bound orbits account for the steepening slopes of the curves $\langle \Delta v_\perp \rangle(\chi)$ seen in Fig. 6 for $\chi \gtrsim 0.7$.

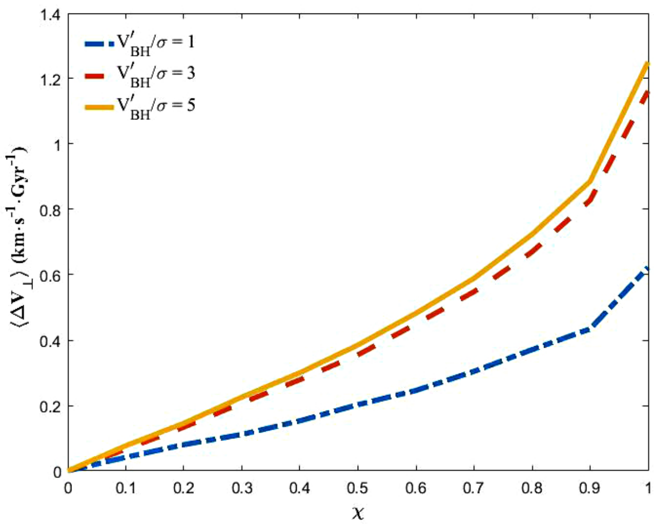

FIG. 6. The coefficient of dynamical friction $\langle \Delta v_\perp \rangle$ as a function of the dimensionless black-hole spin χ for $\theta_S = \pi/2$ and our fiducial parameters $n = 10^6$ pc^{-3}, $m_* = M_\odot$, and $M = 10^6\ M_\odot$. The three curves show three different choices for the ratio between the black-hole velocity and stellar velocity dispersion: $v'_{BH}/\sigma = 5$ (solid yellow curve), $v'_{BH}/\sigma = 3$ (dashed red curve), and $v'_{BH}/\sigma = 1$ (dot-dashed blue curve).

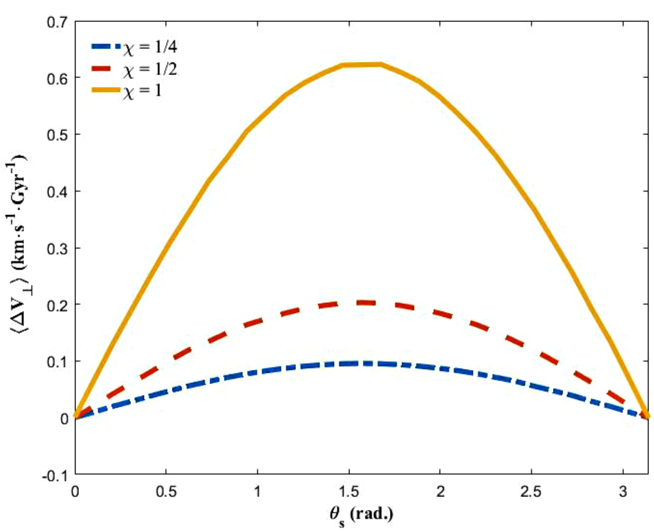

FIG. 7. The coefficient of dynamical friction $\langle \Delta v_\perp \rangle$ as a function of the angle θ_S between the velocity $\mathbf{v'}_{BH}$ and spin $\mathbf{S}$ of the black hole for the same fiducial parameters listed in the caption to Fig. 6. The three curves show three different choices for the dimensionless spin magnitude: $\chi = 1$ (solid yellow curve), $\chi = 1/2$ (dashed red curve), and $\chi = 1/4$ (dot-dashed blue curve).

Fig. 7 shows how the coefficient of gravitomagnetic dynamical friction $\langle \Delta v_\perp \rangle$ depends on the angle θ_S between the velocity $\mathbf{v'}_{BH}$ and spin $\mathbf{S}$ of the black hole. The axisymmetry of the system when $\mathbf{v'}_{BH}$ and $\mathbf{S}$ are parallel ($\theta_S = 0$ or π) implies that the coefficient must vanish for these values. The symmetry of geodesics reflected through the equatorial plane perpendicular to the black-hole spin implies that the coefficient must be symmetric under reflection through this plane ($\theta_S \to \pi/2 - \theta_S$). The combination of these two properties suggests that the direction of the gravitomagnetic dynamical friction force is parallel to $\hat{\mathbf{v}} \times \hat{\mathbf{S}}$ like the Lorentz force law $\mathbf{F} = q\mathbf{v} \times \mathbf{B}$, even if it is not strictly linear in the magnitudes of $\mathbf{v}$ or $\mathbf{S}$ as indicated by Figs. 5 and 6.

Gravitomagnetic friction described by the force law $\mathbf{F} = C\mathbf{v} \times \mathbf{S}$, where

$$C = \frac{M\langle \Delta v_\perp \rangle}{vS\sin\theta_S}\ , \tag{25}$$

would cause a black hole to move on a helical orbit about an axis parallel to its spin $\mathbf{S}$, just as the Lorentz force law causes a charged particle to move on a helix about the magnetic field. The radius of this helix would be

$$R = \frac{Mv\sin\theta_S}{CS} = \frac{(v\sin\theta_S)^2}{\langle \Delta v_\perp \rangle}\ . \tag{26}$$

For $v \simeq 100$ km/s and $\langle \Delta v_\perp \rangle$ given by Eq. (19), $R \simeq 10\,\mathrm{Mpc}$, far larger than any stellar system with a density as high as $n = 10^6\,\mathrm{pc}^{-3}$. A black hole moving on a circular orbit with orbital angular momentum $\mathbf{L}$ will experience an orbit-averaged torque

$$\frac{d\mathbf{L}}{dt} = -\frac{C}{2M}\mathbf{S} \times \mathbf{L} = \boldsymbol{\Omega}_p \times \mathbf{L} \tag{27}$$

implying that $\mathbf{L}$ will precess about $\mathbf{S}$ with a period $\tau_p = 2\pi/\Omega_p \simeq 100\,\mathrm{Gyr}$ for our fiducial parameters, far longer than the dynamical-friction time [35]

$$\begin{aligned} T_{df} &= \left| \frac{v}{\langle \Delta v_\parallel \rangle} \right| = \frac{3}{8}\sqrt{\frac{2}{\pi}} \frac{\sigma^3}{G^2 M n m_* \ln\Lambda} \\ &\simeq 1.6 \times 10^3\,\mathrm{yr} \end{aligned} \tag{28}$$

for our fiducial parameters and $v \ll \sigma$.

V. DISCUSSION

This paper introduces the concept of gravitomagnetic dynamical friction, a component of dynamical friction perpendicular to both the velocity and spin of a supermassive black hole traveling through a stellar background. This force results from the spin-dependent gravitational scattering of stars on hyperbolic orbits in general relativity. We calculate the coefficient of gravitomagnetic dynamical friction $\langle \Delta v_\perp \rangle$ numerically using apsidal and nodal precession at 1.5PN order given by Eq. (7) and the exact spin-dependent angular-momentum threshold for direct capture. We also provide a reasonable analytical estimate of this effect in Eq. (19) based on the assumption supported by our Monte-Carlo simulations that gravitomagnetic dynamical friction is produced by scattering stars with $L \sim GM/c$ where relativistic effects are significant. This estimate suggests that our new coefficient $\langle \Delta v_\perp \rangle$ is suppressed by a factor $(\sigma/c)^2$ compared to the Newtonian coefficient of dynamical friction $\langle \Delta v_\parallel \rangle$ anti-aligned with the black-hole velocity $\mathbf{v}'_{BH}$. This suppression implies that gravitomagnetic dynamical friction will be negligible in galactic systems where $v'_{BH}, \sigma \sim$ 100 km/s and $(\sigma/c)^2 \sim 10^{-7}$. However, the limiting behavior of our estimate shown by Eq. (24) suggests that as the black-hole velocity becomes relativistic ($v'_{BH} \to c$), the two coefficients become comparable and therefore our new effect could be relevant to a black hole interacting with a photon background, circumbinary disk, or relativistic plasma [30–32]. Even in the absence of an immediate application to such a system, it is interesting to consider this qualitatively new dynamical effect introduced by black-hole spin interacting with a collisionless many-body system in general relativity.

ACKNOWLEDGMENTS

We thank Juan Servin for sharing a program to calculate the angular momentum $L_{\rm mb\pm}$ of marginally bound orbits as a function of black-hole spin. M. K. is supported by Alfred P. Sloan Foundation Grant No. RG-2015-65299 and NSF Grant No. PHY-1607031.

[1] S. Chandrasekhar, ApJ **97**, 255 (1943).
[2] J. Binney and S. Tremaine, *Galactic Dynamics: Second Edition, by James Binney and Scott Tremaine. ISBN 978-0-691-13026-2 (HB).* (Princeton University Press, 2008).
[3] T. Murai and M. Fujimoto, PASJ **32**, 581 (1980).
[4] D. N. C. Lin and D. Lynden-Bell, MNRAS **198**, 707 (1982).
[5] R. A. Ibata and G. F. Lewis, ApJ **500**, 575 (1998), astro-ph/9802212.
[6] L. Spitzer, Jr., ApJ **158**, L139 (1969).
[7] J. N. Bahcall and R. A. Wolf, ApJ **216**, 883 (1977).
[8] C. S. Frenk, A. E. Evrard, S. D. M. White, and F. J. Summers, ApJ **472**, 460 (1996), astro-ph/9504020.
[9] J. Dubinski, ApJ **502**, 141 (1998), astro-ph/9709102.
[10] E. C. Ostriker, ApJ **513**, 252 (1999), astro-ph/9810324.
[11] P. Goldreich, Y. Lithwick, and R. Sari, ARA&A **42**, 549 (2004), astro-ph/0405215.
[12] E. Grishin and H. B. Perets, ApJ **811**, 54 (2015), arXiv:1503.02668 [astro-ph.EP].
[13] M. C. Begelman, R. D. Blandford, and M. J. Rees, Nature **287**, 307 (1980).
[14] G. D. Quinlan, New A **1**, 35 (1996), astro-ph/9601092.
[15] M. Milosavljević and D. Merritt, ApJ **563**, 34 (2001), astro-ph/0103350.
[16] F. Antonini and D. Merritt, ApJ **745**, 83 (2012), arXiv:1108.1163.
[17] J. A. González, M. Hannam, U. Sperhake, B. Brügmann, and S. Husa, Physical Review Letters **98**, 231101 (2007), gr-qc/0702052.
[18] M. Campanelli, C. O. Lousto, Y. Zlochower, and D. Merritt, Physical Review Letters **98**, 231102 (2007), gr-qc/0702133.
[19] M. Campanelli, C. Lousto, Y. Zlochower, and D. Merritt, ApJ **659**, L5 (2007), gr-qc/0701164.
[20] A. Gualandris and D. Merritt, ApJ **678**, 780 (2008), arXiv:0708.0771.
[21] J. M. A. Danby and G. L. Camm, MNRAS **117**, 50 (1957).
[22] A. J. Kalnajs, in *IAU Colloq. 10: Gravitational N-Body Problem*, Astrophysics and Space Science Library, Vol. 31, edited by M. Lecar (1972) p. 13.
[23] W. A. Mulder, A&A **117**, 9 (1983).
[24] R. P. Kerr, Physical Review Letters **11**, 237 (1963).
[25] A. Einstein, Sitzungsberichte der Königlich Preußischen Akademie der Wissenschaften (Berlin), Seite 831-839. (1915).
[26] J. Lense and H. Thirring, Physikalische Zeitschrift **19** (1918).
[27] A. Papapetrou, Proceedings of the Royal Society of London Series A **209**, 248 (1951).
[28] B. M. Barker and R. F. Oconnell, General Relativity and Gravitation **11**, 149 (1979).
[29] E. P. Lee, ApJ **155**, 687 (1969).
[30] D. Syer, MNRAS **270**, 205 (1994), astro-ph/9404063.
[31] E. Barausse, MNRAS **382**, 826 (2007), arXiv:0709.0211.
[32] O. J. Pike and S. J. Rose, Phys. Rev. E **89**, 053107 (2014).
[33] L. E. Kidder, Phys. Rev. D **52**, 821 (1995), gr-qc/9506022.
[34] B. Carter, Physical Review Letters **26**, 331 (1971).
[35] D. Merritt, *Dynamics and Evolution of Galactic Nuclei, by David Merritt. ISBN 978-0-691-15860-0.* (Princeton University Press, 2013).
[36] R. Geroch, Journal of Mathematical Physics **11**, 2580 (1970).
[37] R. O. Hansen, Journal of Mathematical Physics **15**, 46 (1974).
[38] J. M. Bardeen, W. H. Press, and S. A. Teukolsky, ApJ **178**, 347 (1972).